

# Computational Modelling of Self-Assembly Behaviour in Nanogel Formation Using Monte Carlo Simulation

H. Cheon<sup>a</sup>, A. H. Jarmund<sup>a</sup>, T. Skjong<sup>a</sup>

<sup>a</sup>*Norges Teknisk-Naturvitenskapelige Universitet, Trondheim, Norway.*

November 2017

---

## Abstract

Recent research has found that attaching Cholesterol groups to Xyloglucan induces self-assembly behaviour, eg. making it potentially useful for drug-carrying. Similar behaviour was found using Monte Carlo simulations. It was, however, found that the concentration of Cholesterol had to reach a lower threshold for self-assembly to occur. Further studies are required to investigate the exact nature of such a threshold and whether there exists any upper concentration limit.

---

## 1. Introduction

Nanogels are nano-sized hydrogel particles (diameter <100nm) [1]. A hydrogel is a cross-linked polymer network that has a large capacity to swell by incorporating water into its network structure [2]. This ability to take up large amounts of water and to incorporate bioactive compounds while remaining relatively stable has made nanogels a candidate for use as drug delivery systems [3].

Nanogels may be divided into two categories based on their cross-linking structure [1]. In chemically cross-linked gels the cross-links are formed via covalent bonding. For physically cross-linked gels the cross-links are formed by non-covalent bonds, such as hydrogen bonds, ionic bonds, or hydrophobic interactions. The production method for nanogels may also be divided into two main categories. Either a precursor polymer which self-assembles into a gel structure is used or gel structure is achieved via heterogeneous polymerisation of monomers where polymerisation and gel formation happens simultaneously. Physical cross-links are normally formed by the self-assembly method whereas a chemically cross-linked gel may be formed with either method [4].

For use in biomedical applications physically cross-linked gels have the advantage that toxic cross-links, catalyst, or by-products are not needed in the production process [1]. For this use polysaccharides have been a favoured choice as backbone polymer. This is due to their biocompatibility and availability [3] as well as their biodegradability [5]. If the backbone chain is modified with hydrophobic groups then they create physical cross-links of hydrophobic domains where hydrophobic drugs may be complexed within the gel [3].

### 1.1. Motivation

This paper focuses on the work undertaken by Sawada et al. [5] as presented in the article: “Self-assembled nanogel of cholesterol-bearing Xyloglucan as a drug delivery

*Preprint submitted to Rita de Sousa Dias*

*November 2017*

nanocarrier". Here the self-assembly behaviour of Xyloglucan, a branched polysaccharide, with Cholesterol groups attached to its side chains was experimentally examined. The hydrophobic Cholesterol side groups drive the self-assembly behaviour for this nanogel. Xyloglucan was noted to be of particular interest as the main chain due to its Galactose side chains which increase water solubility and enable targeted drug delivery by interaction with cell receptors.

Sawada et al. [5] found that increasing the number of Cholesterol groups attached to the Xyloglucan led to a decrease in the diameter of the nanoparticles formed. In our study, it is attempted to reproduce this result using Monte Carlo simulations. Simulations of main chains with one or two side groups of Cholesterol are presented. The end-to-end distance ( $R_{ee}$ ), radial distribution function(RDF), the radius of gyration ( $R_g$ ), and their root-mean-square values are used to compare the simulations. A simulation of a main chain without any side group is also used as a control.

## 2. Method and models

### 2.1. System : Schematic analysis of molecules

In this system, Xyloglucan (XG) and the Cholesterol group (CH) molecules are considered as simulated molecules and this compound is called Cholesterol-bearing Xyloglucan (CHXG). The monomers of the molecule are represented as spherical beads in the simulation.

XG consists of 3 different types of sugar molecules, Glucose, Xylose and Galactose with molar ratio of 45:38:17 respectively [5]. These three types of sugar molecules make up XG main chain and branched side chain. In this simulation all three sugar monomers are considered as identical in terms of mass and radius. 4

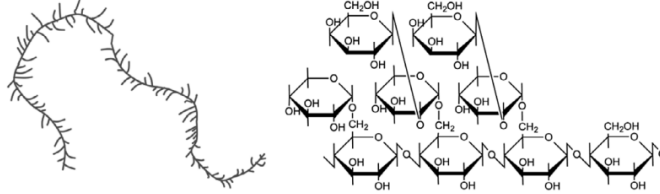


**Figure 1:** The structure of a XG polymer consisting of three types of sugars, which is described as a multi-branched polysaccharide[5]

The Cholesterol group (CH) is functionalised in the XG polysaccharide chain by synthesizing cholesteryl N-(6-isocyanatohexyl) carbamate and XG. CH is made up of two parts, one is Hexamethylenediamine carbamate (HDC), which can be shown as a saturated hydrocarbon chain, and the other is cycloalkane, see Figure 2. The CH is modelled as consisting of two identical beads. 4.

To identify the type of chains in each simulation the same labelling convention as used by Sawada et al. [5] was adopted . The main XG chain without CH (control group)

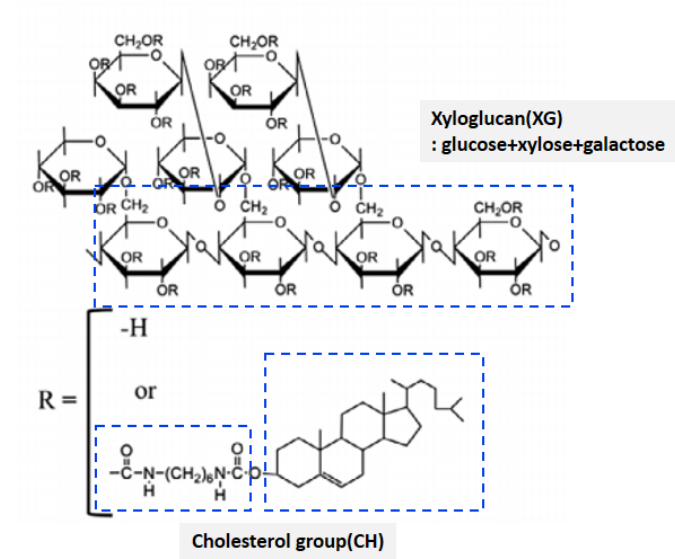


**Figure 2:** The structure of Cholesterol bearing Xyloglucan(CHXG). The two dotted boxes show in blue show each part represented by a bead in the simulation.[5]

was labelled as 'XG'. XG with one CH monomer was labelled 'CHXG1' and XG with two CH monomers was labelled 'CHXG2'.

The outcome of the simulations is expected to be visually similar to the results presented by [5]. Transmission electron microscope(TEM) images of their results can be seen in Figure 3.

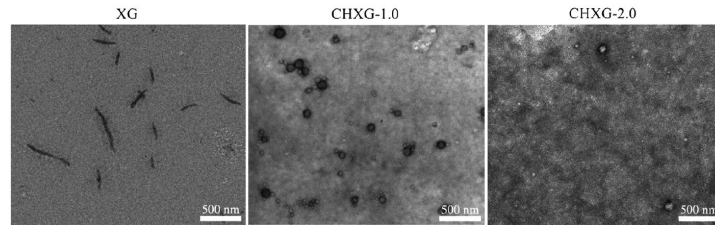


**Figure 3:** TEM images of XG polymers with different concentration of CH. From left to right: the XG polymers without CH look like a rod-shaped compound. CHXG-1.0 and 2.0 have assembled into a spherical shape, though details of the degree of self-assembly cannot be quantified from these images.[5].

## 2.2. Simulation model

Coarse-grained (CG) simulation was used in our study with Molsim software and CG sites were assigned to two different monomers which were mentioned above, XG and CH [6]. In case of one polymer, a long main chain had sites with XG, and short branches which were attached to main chain had sites with XG and CH as illustrated in Figure 5.

In terms of statistical method, there are three modes, molecular dynamics(MD), brownian dynamics(BD), and Monte Carlo(MC), and MC was used in our study.

### 2.3. Energy potential

The hydrophobic interactions were simulated by introducing a Van der Waals force between the Cholesterol monomers in the form of a Lennard-Jones potential(L-J potential) [2],

$$V(r) = 4\epsilon \left[ \left( \frac{\sigma}{r} \right)^{12} - \left( \frac{\sigma}{r} \right)^6 \right] \quad (1)$$

In this study, parameters  $\epsilon = 2.48$  and  $\sigma = 6.00$  were used for L-J potential equation. A plotted graph of L-J potential is Figure 4.

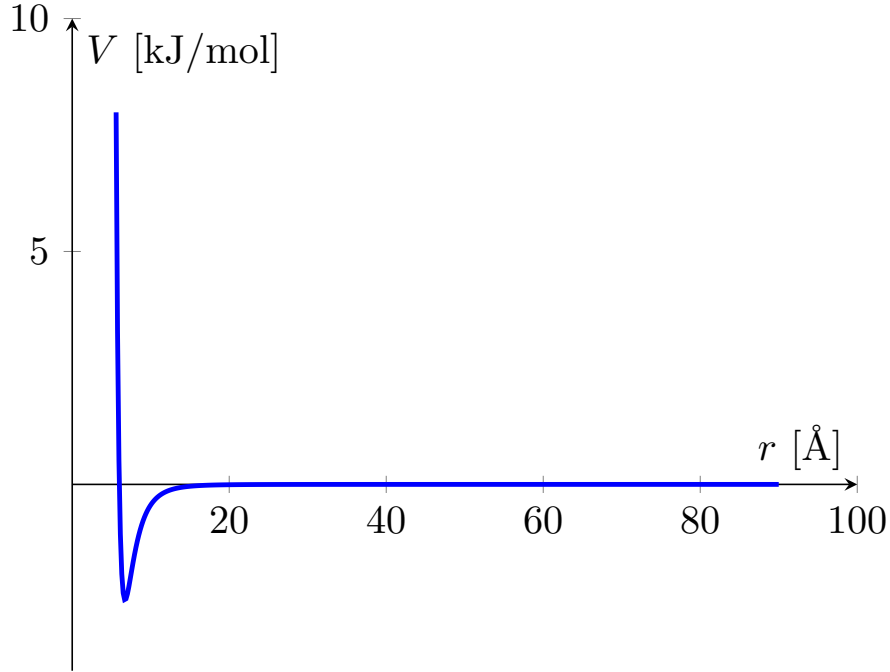


**Figure 4:** A plot of Lennard-Jones potential of simulation with XG and CH( $\epsilon = 2.48$ ,  $\sigma = 6.00$ ). The Van der Waals radius corresponds to 6.73 and L-J potential has the minimum value at  $r = 6.73$ .

### 2.4. Parameters for simulation

A sketch of the polymer is shown in Figure 5 with corresponding parameters given in Table 1 and 2. The experimental parameters are kept constant between experiment are listed in Table 1, whereas those varied are listed in Table 2. See [Appendix A](#), [Appendix B](#) and [Appendix C](#) for the input files. The basic template was a kindly provided gift by associate professor Rita de Sousa Dias.

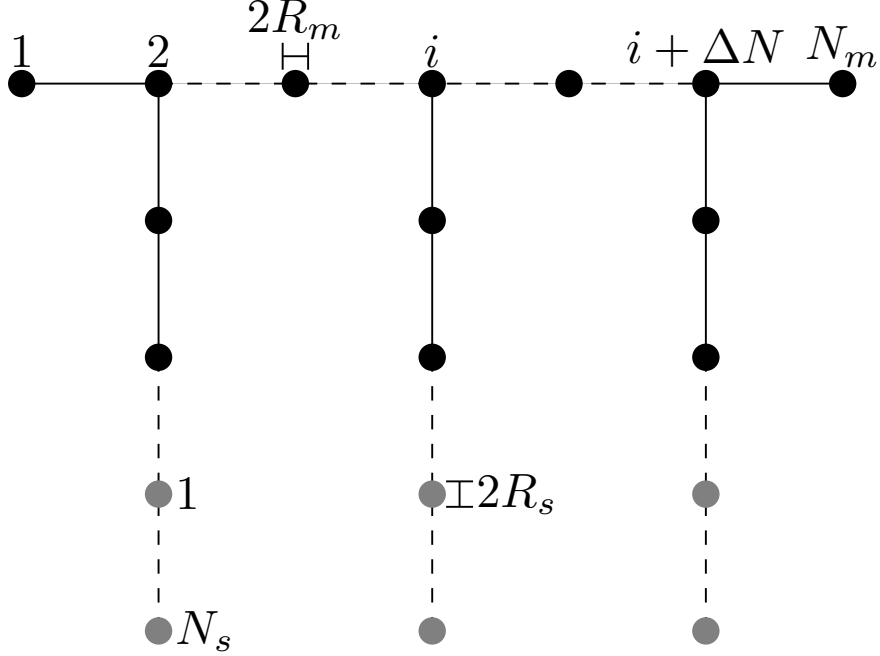


**Figure 5:** A sketch of a coarse-grained polymer as used in this paper. The main chain consists of  $N_m$  monomers with a radius  $R_m$ . The side chains were placed at every  $\Delta N$  monomer in the main chain. Each side chain consists of two sugar-monomers (equal to the main chain monomers) and  $N_s$  non-sugar-monomers representing Cholesterol with a radius  $R_s$ .

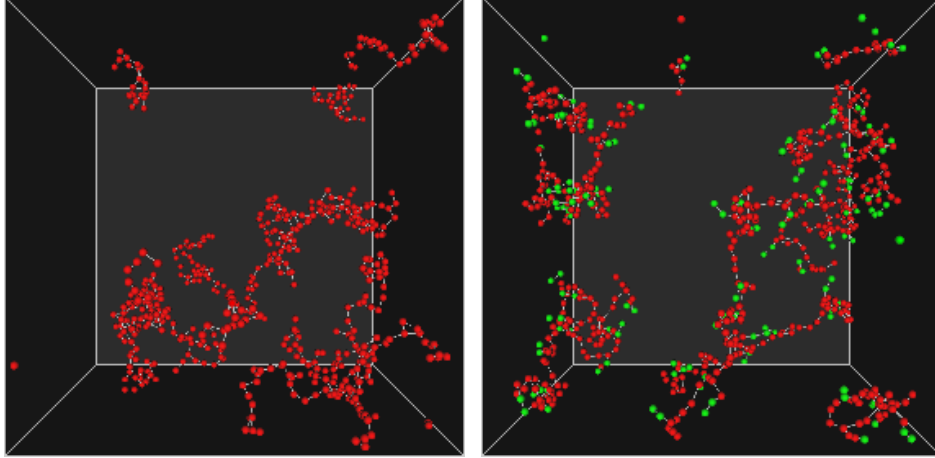
### 3. Results

Simulations were carried out as described in the [Method and models](#) section. Snapshots of the final configurations, assumed to be in equilibrium states, for XG, CHXG1 and CHXG2 are shown in [Figure 6a](#), [6b](#) and [6c](#) respectively. Simulation running times (total CPU time) were 5.27 h for XG, 8.10 h for CHXG1 and 6.88 h for CHXG2.

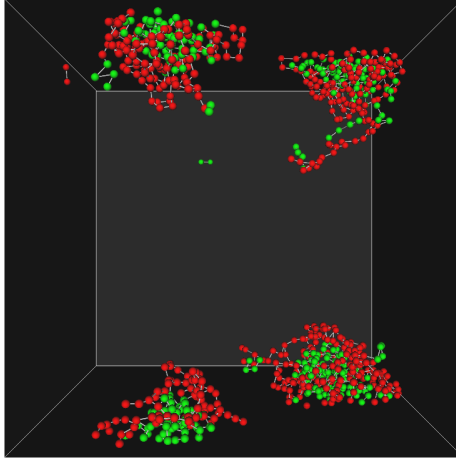
End-to-end radii and radii of gyration are given as root-mean-square (rms) values in [Table 3](#) and their distributions are given in [Figure 7](#) and [Figure 8](#) respectively. Relative difference in rms end-to-end radii compared to XG, which should show no self-assembly, are also given in [Table 3](#).

### 4. Discussion

The results of the simulations show that a chain with two CH molecules show clear self-assembly behaviour. However, this does not appear in the control group (XG) or in the CHXG1, as demonstrated by the relative difference in end-to-end radius  $\delta$  in [Table 3](#) increasing by a factor 100 for CHXG2 compared to CHXG1. This shows that increasing the number of CH induces self-assembly, but that there appears to be a lower limit that must be reached before the interactions of the side chains are strong enough to induce



(a) Snapshot of XG, consisting solely of sugars. (b) Snapshot of CHXG1, consisting of sugars and one cholesterol group.



(c) Snapshot of CHXG2, consisting of sugars and two cholesterol groups.

**Figure 6:** Snapshots of the the final configurations of the simulated polymers, assumed to be in equilibrium states. 8 polymers with main chains of sugars (red beads) and cholesterol groups (each group consisting of two green beads) are shown with periodic boundary conditions. The sugars do not interact whilst the cholesterol groups obey a Lennard-Jones potential to mimic hydrophobic interactions, as described in the [Method and models](#) section.

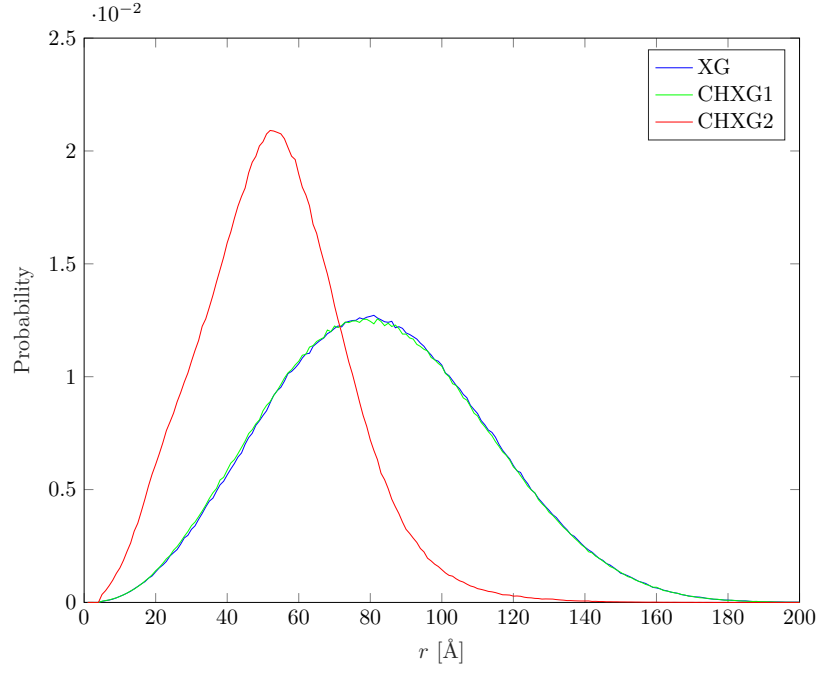


**Figure 7:** Distribution of end-to-end radius for the main chains.

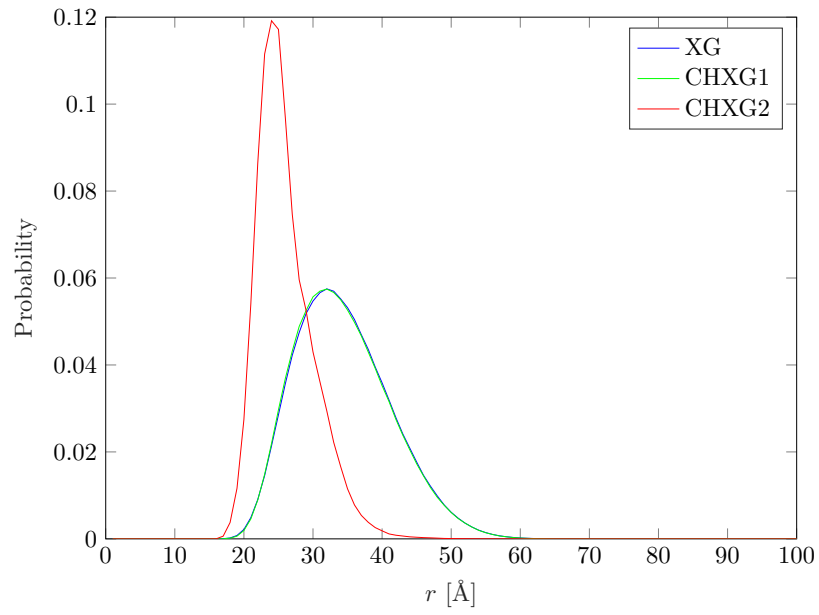


**Figure 8:** Distribution of radius of gyration for the main chains.

**Table 1:** Experimental parameters kept constant in each simulation. Some of the parameters are illustrated in Figure 5. The parameters changed are listed in Table 2.

Parameter	Value	Description
$N_p$	8	# polymers/main chains
$N_m$	50	# monomers in main chain
$\Delta N$	5	# monomers in the main chain between each branch
$R_m$	2 Å	Radius of monomers in main chain
$R_s$	2 Å	Radius of monomers in side chain
$M_m$	10 Da	Molecular weight of monomers in main chain
$M_s$	10 Da	Molecular weight of non-sugar monomers in side chain
$N_{tot,m}$	560	total number of monomers(XG) in main chain
$\sigma$	2.48	$\sigma$ -parameter for the Lennard-Jones potential
$\epsilon$	6.00	$\epsilon$ -parameter for the Lennard-Jones potential
$n_{sim}$	20	# macrosteps
$n_{steps}$	20 000	# iterations in each simulation

**Table 2:** The experimental parameters changed for each simulation; The number of non-sugar monomers in side chain is  $N_s$  and total number of non-sugar monomers (CH) in side chain is  $N_{tot,s}$ . In addition, the parameters listed in Table 1 are kept constant.

	$N_s$	$N_{tot,s}$
XG	0	0
CHXG1	1	160
CHXG2	2	320

self-assembly. The presence of only one CH group appears to be too weak to lead to self-assembly. Increasing the concentration of CH beyond two may induce a difference in self-assembly behaviour, but more simulations would be needed to show this.

The distribution functions of  $R_{ee}$  and  $R_g$  shown in Figure 7 and 8 also exhibit similar trends as  $\sqrt{\langle R_{ee}^2 \rangle}$ . The distributions of XG and CHXG1 are close to completely overlapping, while CHXG2 has a more pronounced and narrow peak. This suggests that in addition to the rms values for CHXG2 being smaller, consistent with self-assembly, the variation in polymer extension is less. It seems that entropy is dominating for XG and CHXG1 while enthalpy has gained a more pronounced role for CHXG2 through the Lennard-Jones potential coming into force.

Increasing the concentration of CH may be done simply through increasing the number of monomers in the side chain. Another way to achieve this would be to increase the number of branches (side chains). Referring to Table 1 and Table 2 this would mean changing parameters  $\Delta N$ ,  $N_m$  or  $N_{tot,s}$ .

The accuracy of the model may be improved by looking more closely at the structure of the CH. As described in the [Method and models](#) section we assume that CH is made up of two monomers, which are considered as spherical beads in this model. However, it is experimentally observed that CH is one monomer and that it is planar in shape. The CH could be modelled as one sphere with a larger radius, but this would overestimate



**Table 3:** Root-mean-square values for end-to-end radius  $R_{ee}$  and radius of gyration  $R_g$  for the main chains for the three molecules. The relative difference  $\delta$  for  $R_{rms,ee}$  compared to XG are given as  $\delta = (R_{rms,ee} - R_{rms,ee}(XG))/R_{rms,ee}(XG)$  in %.

	$\sqrt{\langle R_{ee}^2 \rangle}$ [Å]	$\sqrt{\langle R_g^2 \rangle}$ [Å]	$\delta$
XG	87.769 20	34.628 02	0%
CHXG1	87.443 96	34.541 43	-0.37%
CHXG2	56.622 34	25.836 65	-35.49%

the volume occupied by the CH. A solution to this would be to model a flat molecule by a larger group of small beads.

Possible modifications to the CH structure may also be considered. The HDC in the CH is a saturated carbon chain and consists of single bonds between carbon atoms. Changing some of the single covalent bonds into double or triple bonds would make it an unsaturated chain. It is expected that this would result in structural changes and lead to different  $\sqrt{\langle R_g^2 \rangle}$ . This would be modelled by changing parameters for the bond angle in the Molsim software.

In Table 4 empirical data for the simulated molecules are given. The ratios of molecular volume and weight are of order 1 but not equal to 1 which is assumed in the simulations. Taking the differences in volume and mass for the molecules into account may alter the results, maybe making them more in line with the research of Sawada et al. [5]. This would mean changing the sizes and weights of the beads to more accurately represent the structure of XG. These changes could be made alongside the changes to CH suggested earlier to further improve the model.

**Table 4:** Empirical data for the molecules which are used in this simulation [7]. Molar volume by molecular weight ( $M_w$ ) and density are calculated. For the simulations, mass and radius parameters should be related to data in this table.

Monomers Units	Molecules -	$M_w$ g mol <sup>-1</sup>	Density g cm <sup>-3</sup>	Volume cm <sup>3</sup> mol <sup>-1</sup>	Volume Ratio	Radius Ratio
XG	Glucose	180.16	1.54	116.99	4.89	1.70
XG	Xylose	150.13	1.52	98.77	4.62	1.67
XG	Galactose	180.16	1.72	104.74	4.71	1.68
CH	HDC	232.27	0.84	276.51	6.51	1.87
CH	Cholesterol	386.65	1.05	367.54	7.16	1.93

The strength of the Lennard-Jones potential described by eq. (1) influences how the CH groups interact. The corresponding parameter values in this simulation were given by associate professor Rita de Sousa Dias. As she is experienced and well enlightened on such matters, they are assumed to give a faithful representation of the hydrophobic interactions. In future simulations however, the parameters have to match the model used for the CH groups.

The number of iterations in each simulation could be increased to provide better re-

sults. The snapshots in Figure 6 were compared visually to the ones of shorter simulation runs, qualitatively showing similar trends in self-assembly behaviour, i. e. CHXG2 being significantly different from the other two. This is not proof that equilibrium was reached for the simulations reported in this paper, even though it suggests that the major results are consistent with equilibrium states.

## 5. Conclusions

The experimental results presented by Sawada et al. [5] were partly reproduced. The model used was shown to be able to reproduce self-assembly behaviour, but it was found that there is a threshold value for self-assembly behaviour to occur. To complete the aim of comparing the simulations to the experimental results, further simulations would have to be run. Suggestions for parameters of interest for further research affecting the self-assembly behaviour includes the size of molecules, the number of side chains, the length of side chains, the radius and mass of molecules, the strength of the Lennard-Jones potential and also how Cholesterol is modelled.

## Contributions

Study of background knowledge and theory of nanogel and self-assembly is by Tonje Skjong, study of chemical and molecular analysis for simulation parameters is by Hye-jeong Cheon, and conducting simulation and interpreting result data is by Anders H. Jarmund. In addition, discussion, conclusion, formatting and proof-reading are by all of the authors.

Finally, we feel gladly thankful to have an opportunity to investigate the world of nanogel and simulation and give honour to Rita de Sousa Dias.

## References

- [1] Yoshiro Sasaki and Kazunari Akiyoshi. Nanogel engineering for new nanobiomaterials: From chaperoning engineering to biomedical applications. *The Chemical Record*, 10:366–376, 2010. doi: 10.1002/tcr.201000008.
- [2] Rita de Sousa Dias, Stine Nalum Næss, Arne Mikkelsen, and Arnljot Elgsæter. *MOLECULAR BIOPHYSICS - Compendium*. NTNU, 2017.
- [3] Andrew L. Lyon and Michal J. Serpe. *Hydrogel Micro and Nanoparticles*. John Wiley & Sons, 2012.
- [4] Hui Zhang, Yingjie Zhai, Juan Wang, and Guangxi Zhai. New progress and prospects: The application of nanogel in drug delivery. *Material Science and Engineering*, 60:560–568, 2015. doi: <https://doi.org/10.1016/j.msec.2015.11.041>.
- [5] Shin-ichi Sawada, Hiroko Yukawa, Shigeo Takeda, Yoshihiro Sasaki, and Kazunari Akiyoshi. Self-assembled nanogel of cholesterol-bearing xyloglucan as a drug delivery nanocarrier. *Journal of Biomaterials Science*, 28(10–12):1183–1198, 2017. doi: <http://dx.doi.org/10.1080/09205063.2017.1320827>.
- [6] Jurij Reščić and Per Linse. Molsim: A modular molecular simulation software. *Journal of Computational Chemistry*, 36:1259–1274, 2015. doi: <http://dx.doi.org/10.1002/jcc.23919>.
- [7] Sigma-Aldrich. Product information, 2017. URL <https://www.sigmaaldrich.com/sweden.html>.

## Appendix A. Input File: XG

```

! particle id
!           1                               10
!           x x x x x x x x x x
!           11 0 0 16                       0 56
!           0 0                               0
!           0 0           ...               0
!           0 0                               0
!           0 0                               0

&nmlSystem
  txttitle = 'bottle-brush: small and even side-chain
    ↳ distribution',
  txmethod='mc',      txensemb='nvt',      txbc ='xyz',
    ↳ txstart ='setconf',
  nstep1= 10,          nstep2= 1000,
  boxlen= 3*200.0,
  temp  = 298.0,      prsr = 0.1013,
  iseed = 8431,
  lcont =.t.,  laver =.t.,  ldist =.t.,  lgroup=.f.,
    ↳ lstatic=.t.,  limage=.t.,
  itest = 0,  ipart = 1,  iatom = 1,  iaver = 100,  ishow
    ↳ = 1,  iplot = 0,  ilist = 1,
/
&nmlScale
/
&nmlParticle
  lclink      =.true.,
  maxnbondcl  = 1, 1,
  ngen        = 1
  ictgen(0)   = 1,
  ictgen(1)   = 2,
  nbranch     = 10,
  ibbranchpbeg = 3,
  ibbranchpinc = 5,
  nct         = 2,
  txct        ='50-mer1', '2-mer2',
  ncct        = 8,      80,
  npptct(1,1) = 50,  0,
  npptct(1,2) = 2,  0,
  npt         = 2,
  txpt        ='bead1', 'bead2',
  nppt        = 560,    0,
  natpt       = 1,      1,
  txat        ='site1', 'site2',
  massat      = 10.0,   10.0,

```

```

radat = 2.0,          2.0,

sigat(2) = 6.,
epsat(2) = 2.48,

naatpt(1,1) = 1,
txaat(1,1) = 'site1',
naatpt(1,2) = 1,
txaat(1,2) = 'site2',
itestpart = 10,
/
&nmlPotential
relpermitt = 78.4,
txpot(3) = '(1,6,12)',
/
&nmlPotentialChain bond(1) = 1.0, 2, 5.0, bond(2) = 1.0, 2,
    ↪ 5.0, angle(1) = 0.001, angle(2) = 0.0, clink = 2.4,
    ↪ 2, 5.0 /
&nmlSetConfiguration
txsetconf(1) = 2*'hierarchicalrandom',
! nucell(1,1) = 3*1,
! nucell(1,2) = 3*1,
anglemin = 2*120,
! rclow(1:3,1) = 3*-50.0,
! rcupp(1:3,1) = 3*50.0,
! rclow(1:3,2) = 3*-100.0,
! rcupp(1:3,2) = 3*100.0,
itestcoordinate = 1,
/
&nmlMC
pspart = 2*1.0, dtran      = 2*5.0, drot   = 2*20.0,
ppivot = 2*0.5, drotpivot = 2*360.0,
pchain = 2*0.0, dtranchain = 2*5.0,
/
&nmlStatic
istatic=1,
lchaintypedf=.t.,
/
&nmlGroup /
&nmlChainTypeDF vtype(2)=.true., 0.0, 200., 200, vtype(3)=.
    ↪ true., 0.0, 100., 100, /
&nmlIntList inlist = 0, drnlist = 180.0 /
&nmlDist idist=10, vtype(5)=.true., 0.0, 300.0, 301 /
&nmlImage lvrml =.true. /
&nmlVRML txwhen = 'after_macro', /

```

## Appendix B. Input File: CHXG1

```

! particle id
!           1                               10
!           x x x x x x x x x x
!           11 0 0 16                        0 56
!           0 0                               0
!           0 0           ...                0
!           0 0                               0
!           0 0                               0

&nmlSystem
  txttitle = 'bottle-brush: small and even side-chain
    ↳ distribution',
  txmethod='mc',      txensemb='nvt',      txbc = 'xyz',
    ↳ txstart = 'setconf',
  nstep1= 20,          nstep2= 20000,
  boxlen= 3*200.0,
  temp  = 298.0,      prsr = 0.1013,
  iseed = 8431,
  lcont = .t.,  laver = .t.,  ldist = .t.,  lgroup=.f.,
    ↳ lstatic=.t.,  limage=.t.,
  itest = 0,  ipart = 1,  iatom = 1,  iaver = 100,  ishow
    ↳ = 1,  iplot = 0,  ilist = 1,
/
&nmlScale
/
&nmlParticle
  lclink      = .true.,
  maxnbondcl  = 1, 1,
  ngen        = 1
  ictgen(0)   = 1,
  ictgen(1)   = 2,
  nbranch     = 10,
  ibbranchpbeg = 3,
  ibbranchpinc = 5,
  nct         = 2,
  txct        = '50-mer1', '2-mer2',
  ncct        = 8,      80,
  npptct(1,1) = 50,  0,
  npptct(1,2) = 2,    2,
  npt         = 2,
  txpt        = 'bead1', 'bead2',
  nppt        = 560,    160,
  natpt       = 1,      1,
  txat        = 'site1', 'site2',
  massat      = 10.0,    10.0,

```

```

radat = 2.0,          2.0,

sigat(2) = 6.,
epsat(2) = 2.48,

naatpt(1,1) = 1,
txaat(1,1) = 'site1',
naatpt(1,2) = 1,
txaat(1,2) = 'site2',
itestpart = 10,
/
&nmlPotential
relpermitt = 78.4,
txpot(3) = '(1,6,12)',
/
&nmlPotentialChain bond(1) = 1.0, 2, 5.0, bond(2) = 1.0, 2,
    ↪ 5.0, angle(1) = 0.001, angle(2) = 0.0, clink = 2.4,
    ↪ 2, 5.0 /
&nmlSetConfiguration
txsetconf(1) = 2*'hierarchicalrandom',
! nucell(1,1) = 3*1,
! nucell(1,2) = 3*1,
anglemin = 2*120,
! rclow(1:3,1) = 3*-50.0,
! rcupp(1:3,1) = 3*50.0,
! rclow(1:3,2) = 3*-100.0,
! rcupp(1:3,2) = 3*100.0,
itestcoordinate = 1,
/
&nmlMC
pspart = 2*1.0, dtran      = 2*5.0, drot   = 2*20.0,
ppivot = 2*0.5, drotpivot = 2*360.0,
pchain = 2*0.0, dtranchain = 2*5.0,
/
&nmlStatic
istatic=1,
lchaintypedf=.t.,
/
&nmlGroup /
&nmlChainTypeDF vtype(2)=.true., 0.0, 200., 200, vtype(3)=.
    ↪ true., 0.0, 100., 100, /
&nmlIntList inlist = 0, drnlist = 180.0 /
&nmlDist idist=10, vtype(5)=.true., 0.0, 300.0, 301 /
&nmlImage lvrml =.true. /
&nmlVRML txwhen = 'after_macro', /

```

## Appendix C. Input File: CHXG2

```

! particle id
!           1                               10
!           x x x x x x x x x x
!           11 0 0 16                       0 56
!           0 0                               0
!           0 0           ...               0
!           0 0                               0
!           0 0                               0

&nmlSystem
  txttitle = 'bottle-brush: small and even side-chain
    ↪ distribution',
  txmethod='mc',      txensemb='nvt',      txbc = 'xyz',
    ↪ txstart = 'setconf',
  nstep1= 20,          nstep2= 20000,
  boxlen= 3*200.0,
  temp  = 298.0,      prsr = 0.1013,
  iseed = 8431,
  lcont = .t.,  laver = .t.,  ldist = .t.,  lgroup=.f.,
    ↪ lstatic=.t., limage=.t.,
  itest = 0,  ipart = 1,  iatom = 1,  iaver = 100, ishow
    ↪ = 1,  iplot = 0,  ilist = 1,
/
&nmlScale
/
&nmlParticle
  lclink      = .true.,
  maxnbondcl  = 1, 1,
  ngen        = 1
  ictgen(0)   = 1,
  ictgen(1)   = 2,
  nbranch     = 10,
  ibbranchpbeg = 3,
  ibbranchpinc = 5,
  nct         = 2,
  txct        = '50-mer1', '2-mer2',
  ncct        = 8,      80,
  npptct(1,1) = 50,  0,
  npptct(1,2) = 2,   4,
  npt         = 2,
  txpt        = 'bead1', 'bead2',
  nppt        = 560,    320,
  natpt       = 1,      1,
  txat        = 'site1', 'site2',
  massat      = 10.0,   10.0,

```

```

radat = 2.0,          2.0,

sigat(2) = 6.,
epsat(2) = 2.48,

naatpt(1,1) = 1,
txaat(1,1) = 'site1',
naatpt(1,2) = 1,
txaat(1,2) = 'site2',
itestpart = 10,
/
&nmlPotential
relpermitt = 78.4,
txpot(3) = '(1,6,12)',
/
&nmlPotentialChain bond(1) = 1.0, 2, 5.0, bond(2) = 1.0, 2,
↪ 5.0, angle(1) = 0.001, angle(2) = 0.0, clink = 2.4,
↪ 2, 5.0 /
&nmlSetConfiguration
txsetconf(1) = 2*'hierarchicalrandom',
! nucell(1,1) = 3*1,
! nucell(1,2) = 3*1,
anglemin = 2*120,
! rclow(1:3,1) = 3*-50.0,
! rcupp(1:3,1) = 3*50.0,
! rclow(1:3,2) = 3*-100.0,
! rcupp(1:3,2) = 3*100.0,
itestcoordinate = 1,
/
&nmlMC
pspart = 2*1.0, dtran      = 2*5.0,      drot   = 2*20.0,
ppivot = 2*0.5, drotpivot = 2*360.0,
pchain = 2*0.0, dtranchain = 2*5.0,
/
&nmlStatic
istatic=1,
lchaintypedf=.t.,
/
&nmlGroup /
&nmlChainTypeDF vtype(2)=.true., 0.0, 200., 200, vtype(3)=.
↪ true., 0.0, 100., 100, /
&nmlIntList inlist = 0, drnlist = 180.0 /
&nmlDist idist=10, vtype(5)=.true., 0.0, 300.0, 301 /
&nmlImage lvrml =.true. /
&nmlVRML txwhen = 'after_macro', /

```